Pro-inflammatory cells sustain leukemic clonal expansion in T-cell large granular lymphocyte leukemia

Cristina Vicenzetto,[1,2°] Vanessa Rebecca Gasparini,[1,2] Gregorio Barilà,[1,2°] Antonella Teramo,[1,2] Giulia Calabretto,[1,2] Elisa Rampazzo,[1,2] Samuela Carraro,[1°] Valentina Trimarco,[1] Livio Trentin,[1] Monica Facco,[1,2] Gianpietro Semenzato[1,2] and Renato Zambello[1,2]

[1]Department of Medicine, Hematology and Clinical Immunology Branch, University of Padova and [2]Veneto Institute of Molecular Medicine (VIMM), Padova, Italy

°*Current address of CV: Department of Cardiac, Thoracic, Vascular Sciences and Public Health; University of Padova, Padova, Italy.*
°*Current address of GB: Hematology Unit, Ospedale San Bortolo, Vicenza, Italy.*
°*Current address of SC: Department of Medicine, University of Padova, Padova, Italy.*

Correspondence: R. Zambello
r.zambello@unipd.it

Received: November 18, 2022.
Accepted: July 5, 2023.
Early view: July 13, 2023.

https://doi.org/10.3324/haematol.2022.282306

Supplemental Materials

Supplementary Methods

ELISA

Cell culture supernatants were centrifuged to eliminate cellular debris and the level of IL-6 secretion was measured by ELISA kit (RayBiotech and FineTest), following the manufacturer's recommendations and acquired by a microplate reader platform (Victor Multilabel plate reader, PerkinElmer). The induction of secretion after stimulation was evaluated by normalizing the treated samples with the untreated ones. Complete medium was used as blank control.

Western Blotting analysis

Monocytes were lysed using an in-house lysis buffer. Protein concentration was determined with Bradford method (Sigma Aldrich). A defined amount of extracted proteins was then resuspended in a denaturing loading buffer and was heated at 100°C for 5'. Proteins were resolved, based on their molecular weight (MW), in Dodecyl Sulfate-Polyacrylamide Gel Electrophoresis (SDS-PAGE) and were transferred on poly-vinylidene fluoride membranes (PVDF; Pierce Biotechnology). The membranes were immunostained with monoclonal antibodies and revealed using an enhanced chemiluminescent detection system (ThermoFisher Scientific). The chemioluminescence was acquired with ImageQuant LAS 500 and analyzed by ImageQuant TL v8.1 software (GE Healthcare). The phosphorylation was evaluated by normalizing the optical density of the phosphorylated protein with the one of the total protein. The level of protein expression was normalized over the house keeping protein GAPDH, used as a loading control. For Western blot analysis the following primary or secondary antibodies were used: anti-phospho STAT3 Tyrosine 705 (Cell Signaling, cod. 9145S), anti-STAT3 (Cell Signaling, cod. 4904S), anti-phospho p65 (Cell Signaling, cod. 3031S) , anti-phospho ERK1/2 (Cell Signaling, cod. 4370S), anti-ERK1/2 (Cell Signaling, cod. 9102), anti-p65 (Santa Cruz, cod. Sc-8008), and GAPDH (Millipore MAB374).

RT-qPCR analysis

Total cellular RNA was extracted from cells using the RNeasy Mini Kit (Qiagen) according to the manufacturer's protocol and was treated with DNase (Qiagen). Complementary DNA was generated from 1 mg of total RNA using oligo-dT primer and the AMV reverse transcriptase (Promega). Real-time polymerase chain reaction (RT-PCR) was carried out using QuantStudio5 (ThermoFisher Scientific, Waltham, USA). SYBR Green PCR Master Mix was purchased by NEB (Ipswich, USA). The primers were self-designed and listed below:

- IL-6: forward 5'-GGCACTGGCAGAAAACAACCTG-3', reverse 5'-TCACCAGGCAAGTC TCCTCATTGAAT-3';
- CCL5: forward 5'-TCTGCCTCCCCATATTCCTCGG-3', reverse 5'-GGCGGTTCTTTCGGGTGACAAAG-3';
- CCR5: forward 5'-CAAAAAGAAGGTCTTCATTAC, reverse 5'-CCTGTGCCTCTTCTTCTCATTT-3';
- GAPDH: forward 5'-AATGGAAATCCCATCACCATCT-3' reverse 5'-CGCCCCACTTGATTTTGG-3'.

Standard curves were generated for each gene to evaluate primer efficiency. The relative amounts of messenger RNA (mRNA) were normalized for GAPDH expression and determined by the DDct method.

Statistical analysis

Statistical evaluations were carried out using GraphPad and R softwares. Data were firstly analysed for normal distribution with Kolmogorov-Smirnov test or Shapiro-Wilk test. Statistical significance between two groups was assessed with t-test or Mann-Witney test, according to data distribution. Comparisons between groups were evaluated by one-way ANOVA or Kruskall-Wallis test, based on data distribution. For the analysis of more variable between groups two-way ANOVA test was used with correction for multiple comparisons. For correlation analysis Pearson or Spearman test were used.

Supplemental Table 1

LGLL code	age	Neutropenia	Anemia	Splenomegaly	Thrombocytopenia	OS (y)	AD	Others neoplasias
LGLL149	67	no	no	no	no	8	no	no
LGLL170	68	no	no	no	no	10	no	no
LGLL179	82	no	no	no	no	12	yes	no
LGLL299	67	no	no	no	no	10	no	no
LGLL345	71	yes	yes	no	no	4	no	yes
LGLL434	60	no	no	no	no	3	yes	no
LGLL48	83	no	no	no	no	15	no	no
LGLL557	83	no	no	no	no	2	yes	no
LGLL56	82	no	no	no	no	13	no	yes
LGLL564	45	yes	no	no	no	2	no	no
LGLL92	64	no	no	no	no	15	no	no
LGLL10	61	no	no	no	no	19	no	no
LGLL562	44	no	no	no	no	3	no	no
LGLL665	41	no	no	yes	no	2	NA	NA
LGLL1	56	no	no	no	no	14	no	no
LGLL455	51	no	no	no	no	5	no	no
LGLL5	65	no	no	no	no	14	no	yes
LGLL354	59	no	no	no	no	7	no	no
LGLL280	73	no	no	no	no	9	no	no
LGLL408	83	yes	no	no	no	8	no	no
LGLL141	53	no	no	no	no	11	no	yes
LGLL16	69	yes	no	yes	no	14	no	no
LGLL212	72	yes	no	yes	no	6	no	no
LGLL272	58	yes	no	no	no	5	no	no
LGLL3	52	yes	no	no	no	14	no	no
LGLL41	58	yes	yes	no	no	18	yes	no
LGLL438	83	yes	no	no	no	4	yes	no
LGLL487	75	yes	no	no	no	2	no	no
LGLL547	87	yes	yes	yes	no	1	no	yes
LGLL80	62	yes	no	no	no	10	yes	no
LGLL93	87	yes	yes	no	yes	11	yes	yes
LGLL278	81	no	no	NA	no	5	NA	NA
LGLL254	87	yes	no	no	no	7	yes	no
LGLL685	77	yes	no	no	no	2	no	no
LGLL679	66	yes	no	no	no	2	yes	no
LGLL740	58	yes	yes	yes	no	1	yes	no
LGLL565	61	yes	no	no	no	1	yes	no
LGLL4	74	yes	no	no	no	16	no	no
LGLL904	35	yes	no	no	no	5	no	yes
LGLL20	74	no	no	no	no	18	no	yes
LGLL21	65	no	no	no	no	13	no	no
LGLL258	76	no	no	no	no	9	yes	no
LGLL282	73	no	no	no	no	5	no	no
LGLL416	72	no	no	no	no	4	no	no
LGLL440	65	yes	no	NA	no	4	NA	NA
LGLL58	81	no	no	no	no	13	no	no
LGLL231	85	no	no	no	no	8	no	no
LGLL567	71	no	no	no	no	3	no	no
LGLL32	61	no	no	no	no	13	no	yes
LGLL207	69	no	no	no	no	8	no	no
LGLL74	67	no	no	no	no	14	no	no
LGLL132	77	no	no	no	no	12	no	yes
LGLL146	67	no	no	no	no	12	no	no
LGLL2	80	no	no	yes	no	25	yes	no
LGLL379	74	no	no	no	no	4	no	no
LGLL49	80	no	no	no	no	24	no	yes
LGLL63	90	no	no	no	no	14	no	yes
LGLL259	71	no	no	no	no	5	no	no

Supplemental Table 1: Clinical features of the cohort of patients. OS: overall survival (evaluated at time of the analysis), y: years, AD: autoimmune diseases, NA: not available.

Supplemental Table 2

LGLL code	%LGL	CD4/CD8	Immunophenotype	STAT mutation
LGLL149	66	CD8	CD3+/57 66%; CD3+/CD56+ 56%; CD3+/CD16+ 37%	wt
LGLL170	47	CD8	CD3+/CD57+ 47%; CD3+/CD56+ 15%	wt
LGLL179	46	CD8	CD3+/CD57+ 46%	wt
LGLL299	47	CD8	CD3+/CD57+ 47%	wt
LGLL345	40	CD8	CD3+/CD57+ 40%; CD3+/CD16+ 35%; CD3+/CD56+ 17%	wt
LGLL434	86	CD8	CD3+/CD16+ 86%	wt
LGLL48	75	CD8	CD3+/CD57+/CD56+ 75%	wt
LGLL557	62	CD8	CD3+/CD57+ 62%; CD3+/CD56+ 23%	wt
LGLL56	60	CD8	CD3+/CD57+/CD56+ 60%	wt
LGLL564	34	CD8	CD3+/CD57+ 37%; CD3+/CD16+ 21%	wt
LGLL92	57	CD8	CD3+/CD57+ 57%; CD3+/CD56+ 46%	wt
LGLL10	35	CD8	CD3+/CD57+ 35%; CD3+/CD56+ 26%	wt
LGLL562	45	CD8	CD3+/CD57+ 45%	wt
LGLL665	77	CD8	CD3+/CD57+ 77%	wt
LGLL1	38	CD8	CD3+/CD57+ 38%; CD3+/CD56+ 20%	wt
LGLL455	51	CD8	CD3+/CD57+ 51%; CD3+/CD56+ 38%; CD3+/CD16+ 20%	wt
LGLL5	50	CD8	CD3+/CD57+ 50%	wt
LGLL354	23	CD8	CD3+/CD57+ 23%; CD3+/CD16+ 20%; CD3+/CD56+ 18%	wt
LGLL280	54	CD8	CD3+/CD57+ 54%; CD3+/CD16+ 27%; CD3+/CD56+ 39%	wt
LGLL408	64	CD8	CD3+/CD57+ 64%; CD3+/CD16+ 51%;	wt
LGLL141	26	CD8	CD3+/CD57+ 26%; CD3+/CD16+ 21%	STAT3 D661Y
LGLL16	67	CD8	CD3+/CD57+ 66%; CD3+/CD16+ 60%	STAT3 D661Y
LGLL212	45	CD8	CD3+/CD57+/CD16+ 45%	STAT3 D661Y
LGLL272	57	CD8	CD3+/CD57+/CD16+ 57%	STAT3 D661V
LGLL3	65	CD8	CD3+/CD16+ 65%; CD3+/CD57+ 56%	STAT3 Y640F
LGLL41	88	CD8	CD3+/CD16+ 88%; CD3+/CD57+ 15%	STAT3 D566N
LGLL438	36	CD8	CD3+/CD57+/CD16+ 36%	STAT3 D661Y
LGLL487	85	CD8	CD3+/CD16+ 85%; CD3+/CD57+ 40%	STAT3 D661Y
LGLL547	34	CD8	CD3+/CD57+/CD16+ 34%	STAT3 Y640F
LGLL80	48	CD8	CD3+/CD57+ 48%; CD3+/CD16+ 43%	STAT3 Y640F
LGLL93	51	CD8	CD3+/CD16+ 51%; CD3+/CD57+ 30%	STAT3 N647I
LGLL278	47	CD8	CD3+/CD57+/CD16+/CD56+ 47%	STAT3 Y640F
LGLL254	47	CD8	CD3+/CD16+ 47%; CD3+/CD57+ 36%	STAT3 Y640F
LGLL685	54	CD8	CD3+/CD16+ 56%; CD3+/CD57+ 45%	STAT3 D661Y
LGLL679	60	CD8	CD3+/CD57+/CD16+ 60%	STAT3 N647I
LGLL740	71	CD8	CD3+/CD16+ 71; CD3+/CD57+ 51%	STAT3 Y640F
LGLL565	47	CD8	CD3+/CD57+/CD16+ 47%	STAT3 Y640F
LGLL4	75	CD8	CD3+/CD16+ 75%	STAT3 Y640F
LGLL904	80	CD8	CD3+/CD57+ 80%; CD3+/CD56+ 75%	STAT3 Y640F
LGLL20	77	CD4	CD3+/CD57+/CD56+ 77%	wt
LGLL21	57	CD4	CD3+/CD57+ 57%; CD3+/CD56+ 36%	wt
LGLL258	49	CD4	CD3+/CD57+ 49%; CD3+/CD56+ 44%	wt
LGLL282	50	CD4	CD3+/CD57+ 50%; CD3+/CD56+ 42%	wt
LGLL416	41	CD4	CD3+/CD57+ 41%; CD3+/CD56+ 32%	wt
LGLL440	33	CD4	CD3+/CD57+ 33%; CD3+/CD56+ 29%; CD3+/CD16+ 18%	wt
LGLL58	70	CD4	CD3+/CD57+/CD56+ 70%	wt
LGLL231	64	CD4	CD3+/CD56+ 64%; CD3+/CD57+ 32%	wt
LGLL567	62	CD4	CD3+/CD57+ 62%; CD3+/CD56+ 43%	wt
LGLL32	49	CD4	CD3+/CD56+ 49%; CD3+/CD57+ 45%	wt
LGLL207	62	CD4	CD3+/CD57+ 62%; CD3+/CD56+ 58%	wt
LGLL74	58	CD4	CD3+/CD57+/CD56+ 58%	wt
LGLL132	69	CD4	CD3+/CD57+ 69%; CD3+/CD56+ 49%	STAT5B T628S G452R
LGLL146	57	CD4	CD3+/CD57+ 57%; CD3+/CD56+ 34%	STAT5B S715F
LGLL2	84	CD4	CD3+/CD57+/CD56+/CD16+ 84%	STAT5B T628S
LGLL379	80	CD4	CD3+/CD57+ 80%; CD3+/CD56+ 77%	STAT5B Y665F
LGLL49	50	CD4	CD3+/CD57+ 50%; CD3+/CD56+ 46%	STAT5B N642H
LGLL63	71	CD4	CD3+/CD56+ 71%; CD3+/CD57+ 66%	STAT5B T628S
LGLL259	54	CD4	CD3+/CD57+/CD56+/CD16+ 54%	STAT5B N642H L643M

Supplemental Table 2: Biological features of the leukemic clone in the cohort of patients.

Supplemental Figure 1

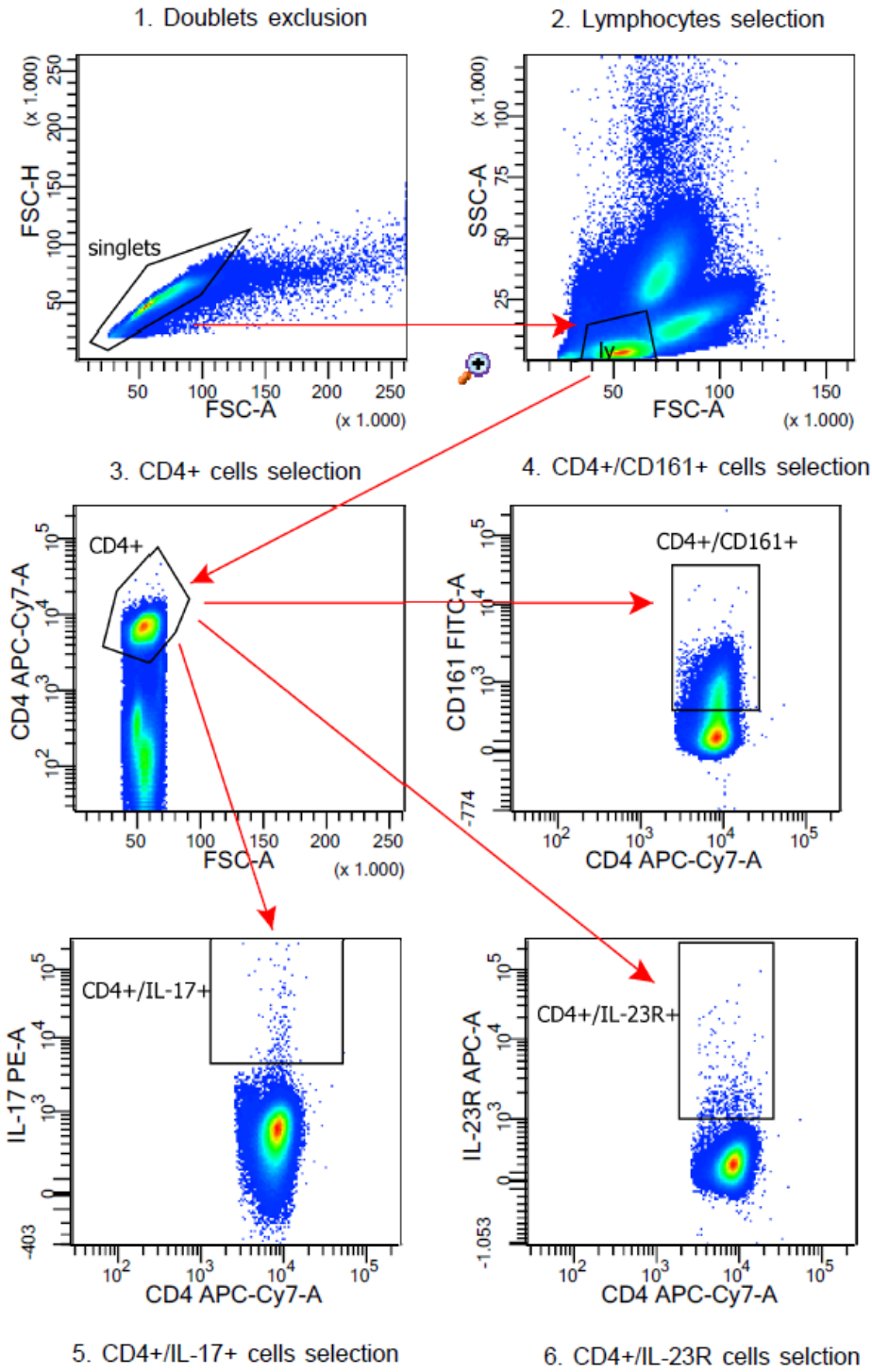

Supplemental Figure 1: Gating strategy for Th17 cells identification. To select lymphocytes based on their morphological features, SSC and FSC parameters were reported in a dot plot cytogram. Lymphocytes gate was set up to select CD4+ lymphocytes based on the high intensity of this antigen expression. To identify Th17 cells, the positivity of CD4+ lymphocytes (on the x axis) and of one of the three antigens, CD161, IL-17 and IL-23R (on the y axis), was evaluated. More in detail, Th17 cells were defined as CD4+/CD161+/IL-17+/IL-23R+. Doublets were excluded through the selection of the population which was positioned at the bisector of the dot plot reporting the two FSC parameters [the relative pick height (H) on the y axis and amplitude (A) at the x].

Supplemental Figure 2

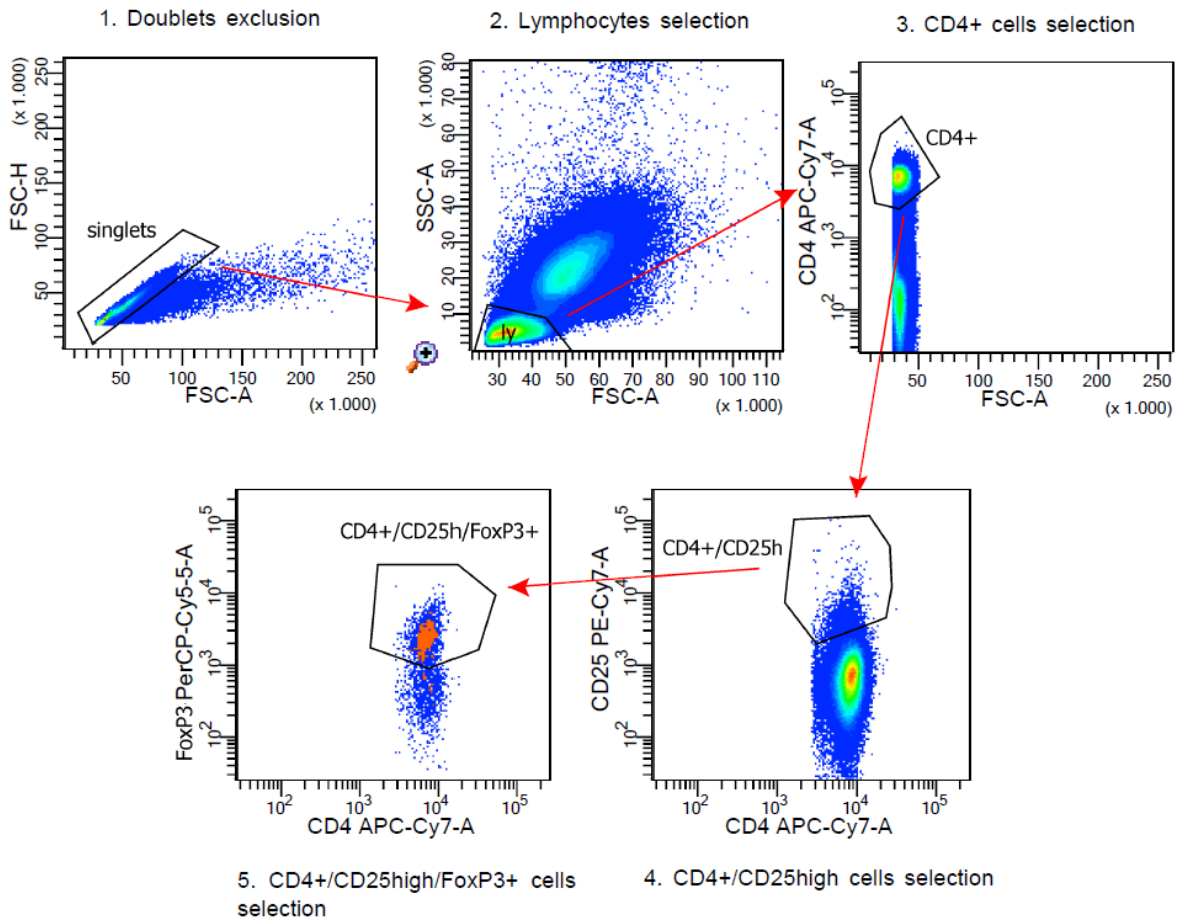

Supplemental Figure 2: Gating strategy for Treg cells identification. SSC and FSC parameters were reported in the following dot plot citograms, in order to select lymphocytes based on their morphological features. Lymphocytes gates were reported in a dot plot to select CD4+ lymphocytes based on the high intensity of this antigen expression. Subsequently, Treg cells were selected by the identification of the CD4+ lymphocytes expressing high level of CD25 and the relative generated gate was then evaluated for intracellular FoxP3 expression. Doublets were excluded through the selection of the population which was positioned at the bisector of the dot plot reporting the two FSC parameters [the relative pick height (H) on the y axis and amplitude (A) at the x].

Supplemental Figure 3

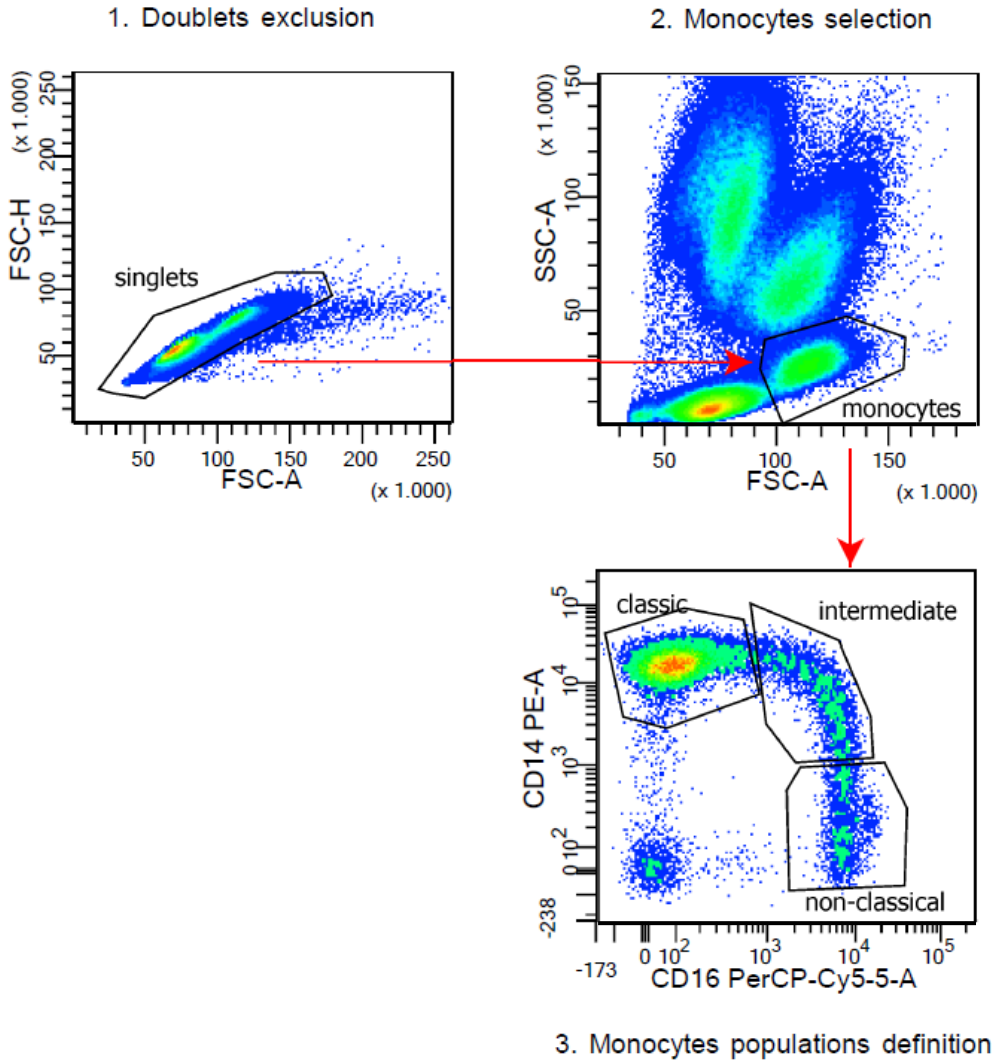

Supplemental Figure 3: Gating strategy used to determine the three monocytes populations. In the following dot plots SSC and FSC parameters were reported, in order to select monocytes based on their morphological features. Lastly monocytes gate was reported in the dot plot which harbours the fluorescence intensity given by the positivity, on the y axis, to CD14 and, on the x axis, to CD16. The three monocytic populations were then selected according to their immunophenotypical features: classic monocytes are defined by the CD14high/CD16- phenotype, intermediate by the CD14+/CD16± phenotype and non-classical by the CD14±/CD16+ phenotype. Doublets were excluded through the selection of the population which was positioned at the bisector of the dot plot reporting the two FSC parameters [the relative pick height (H) on the y axis and amplitude (A) on the x axis].

Supplemental Figure 4

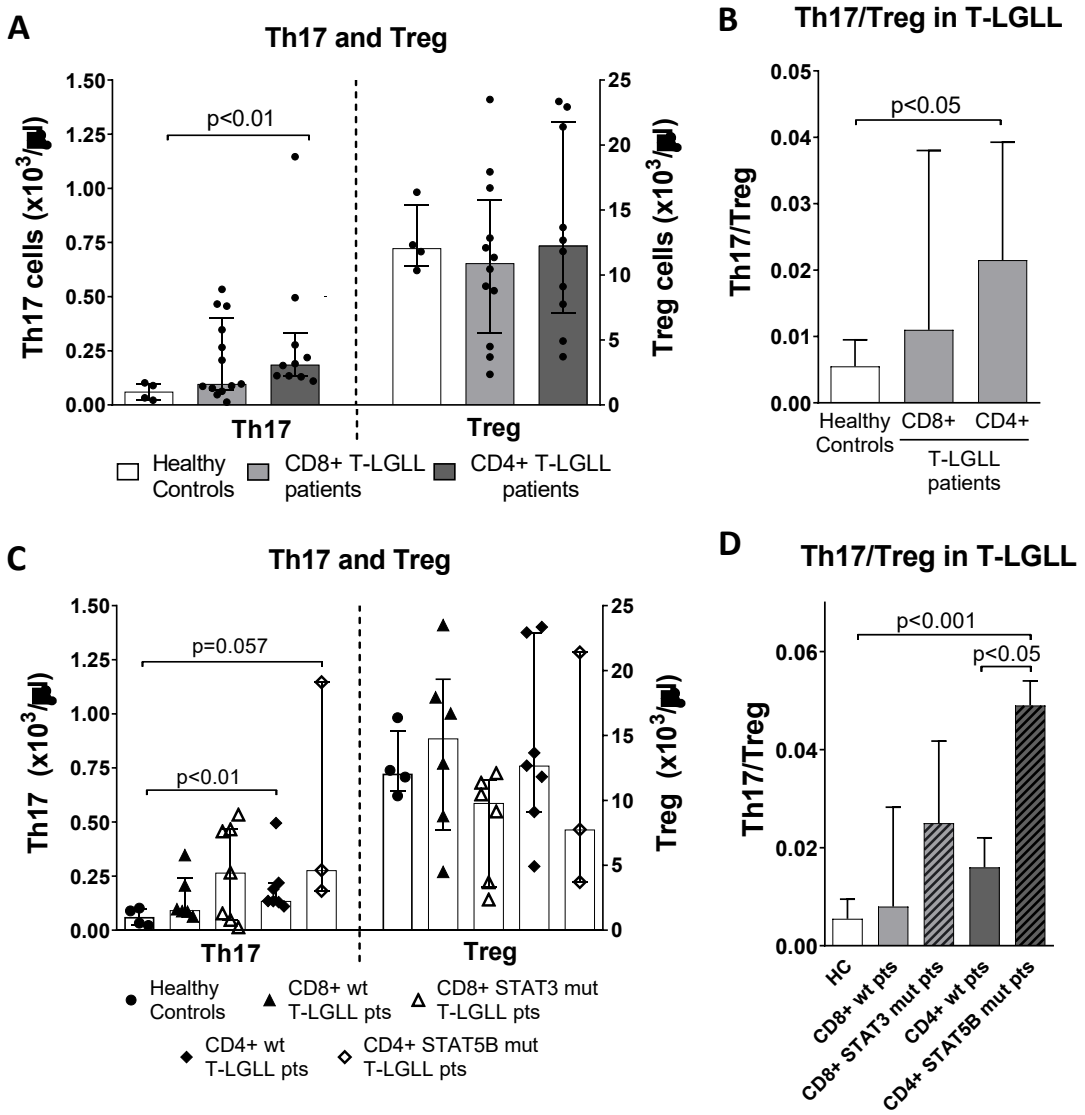

Supplemental Figure 4: Th17 and Treg distribution in T-LGLL patients. The absolute count of Th17 and Treg (panels **A** and **C**) were calculated by flow cytometry on CBC and the related Th17/Treg ratio (panels **B** and **D**) was mathematically set. Kruskal-Wallis corrected for multiple comparisons has been used for the analysis. Data are reported as histograms showing median IQR. (Panels **A-B**) CD8+ and CD4+ T-LGLL patients (n=13 and 10) were characterized by an increase of Th17 cells. Th17/Treg ratio was imbalanced for CD4+ cases in comparison to healthy controls (n=4). (panels **C-D**) The increased Th17 cells characterized either CD4+ wt (n=7) and *STAT5B* mutated (n=3) patients (pts), leading to a significant skewing of the Th17/Treg ratio in these groups.

Supplemental Figure 5

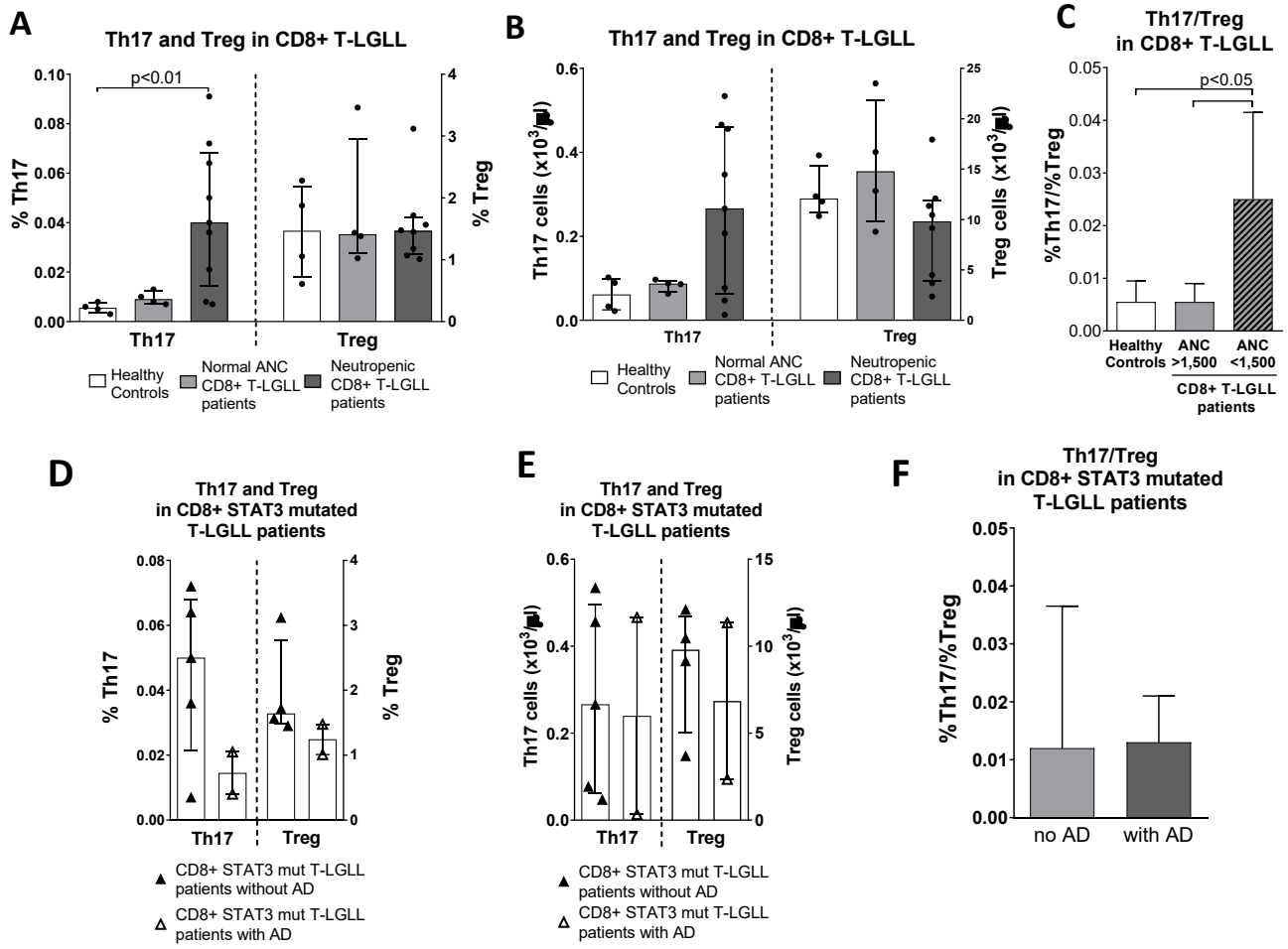

Supplemental Figure 5: Th17 and Treg distribution in neutropenic T-LGLL patients . The percentage of Th17 and Treg (panels **A, D**) were evaluated by flow cytometry; the related ratio (panels **C, F**) and the absolute Th17 and Treg count were mathematically set (panels **B, E**). Kruskal-Wallis test has been used for the analysis. Data are reported as histograms showing median IQR. (**A-C**) CD8+ neutropenic T-LGLL patients [Absolute Neutrophils Count (ANC) <1,500, n=8] were characterized by an increase of Th17 cells, leading to an imbalanced Th17/Treg ratio in comparison to CD8+ non-neutropenic T-LGLL patients (ANC>1,500; n=4) and healthy controls (n=4). (panels **D-F**). CD8+ *STAT3* mutated T-LGLL patients with concomitant autoimmune diseases (AD; n=2) were characterized by similar Th17 and Treg cells percentages, and related ratio, with cases without AD (n=5).

Supplemental Figure 6

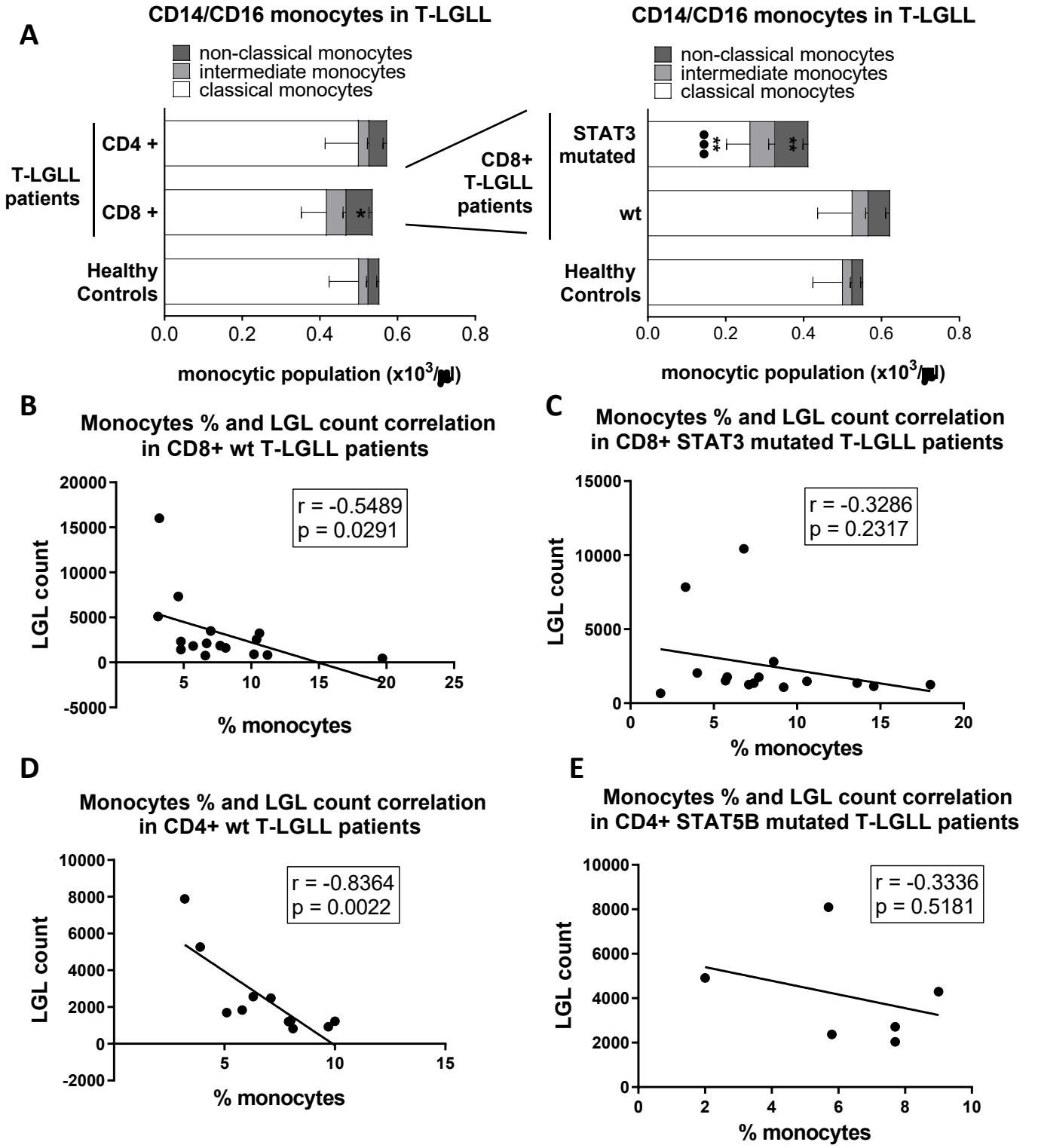

Supplemental Figure 6: Monocytes distribution in peripheral blood of T-LGLL patients. (**A-B**) The absolute count of classic, intermediate and non-classic monocyte were calculated by flow cytometry on CBC data. Data are reported as histograms showing mean with SE and have been analyzed by 2-way ANOVA. Increased non-classic monocytes were identified in CD8+ patients (n=17) in comparison to healthy controls (n=5, * = p<0.05), as shown in the left panel (CD4+ cases n=10, **A**). The imbalanced monocytes distribution resulted specific for *STAT3* mutated cases (n=7) in comparison to CD8+ wt ones (n=10, •, **B**) and healthy controls [(*); •••= p<0.001; ** = p<0.01], right panel. (**C-E**) The correlation between the % of monocytes in PB and the leukemic clone count was evaluated in T-LGLL patients' categories (n=17 CD8+ wt, B; n=16 CD8+ *STAT3* mutated, C; n=11 CD4+ wt, D and n=6 CD4+ *STAT5B* mutated) by Spearman analysis. A significant inverse correlation have been identified for CD8+ wt (**B**) and CD4+ wt (**C**) cases.

Supplemental Figure 7

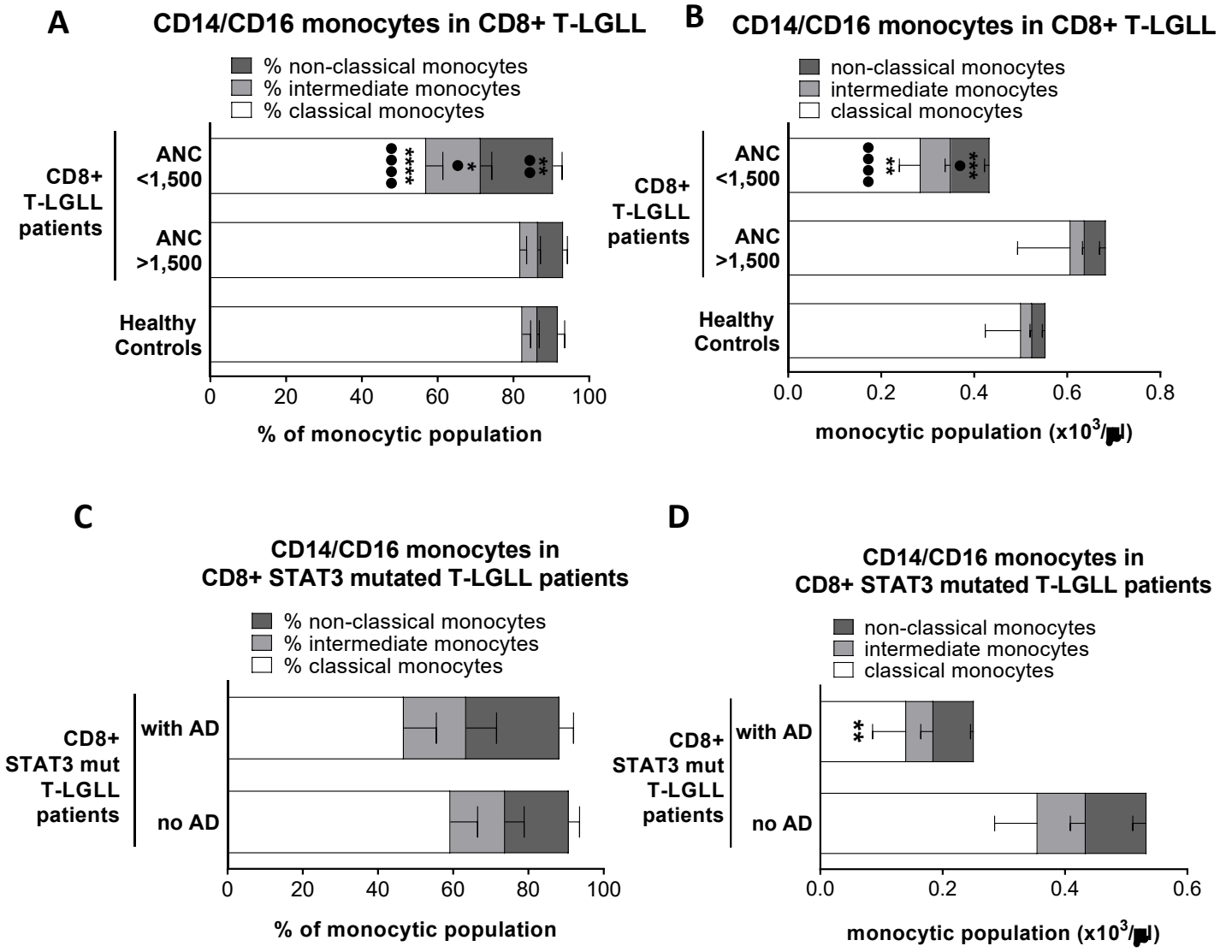

Supplemental Figure 7: Monocytes distribution in peripheral blood of T-LGLL patients. The percentage (panels **A-C**) of classic, intermediate and non-classic monocytes was assessed by flow cytometry; while their absolute count (panels **B-D**) was calculated by flow cytometry in CBC. Data are reported as histograms showing mean with SE and have been analyzed by 2-way ANOVA.(**A-B**) An imbalanced percentage and absolute count of monocytes subtypes was evidenced for CD8+ neutropenic T-LGLL patients [Absolute Neutrophils Count (ANC) <1,500, n=10] in comparison to CD8+ non-neutropenic T-LGLL patients (ANC >1,500; n=7, •) and healthy controls (n=5. (**C-D**) A similar percentage of monocyte populations was evidenced among CD8+ STAT3 mutated T-LGLL patients without (n=4) and with (n=3) autoimmune disease (AD) concurrence, while the absolute classic monocyte count was significantly reduced . •••• and **** = p<0.0001; ***=p<0.001; •• and ** = p<0.01; • and * = p<0.05** = p<0.01.

Supplemental Figure 8

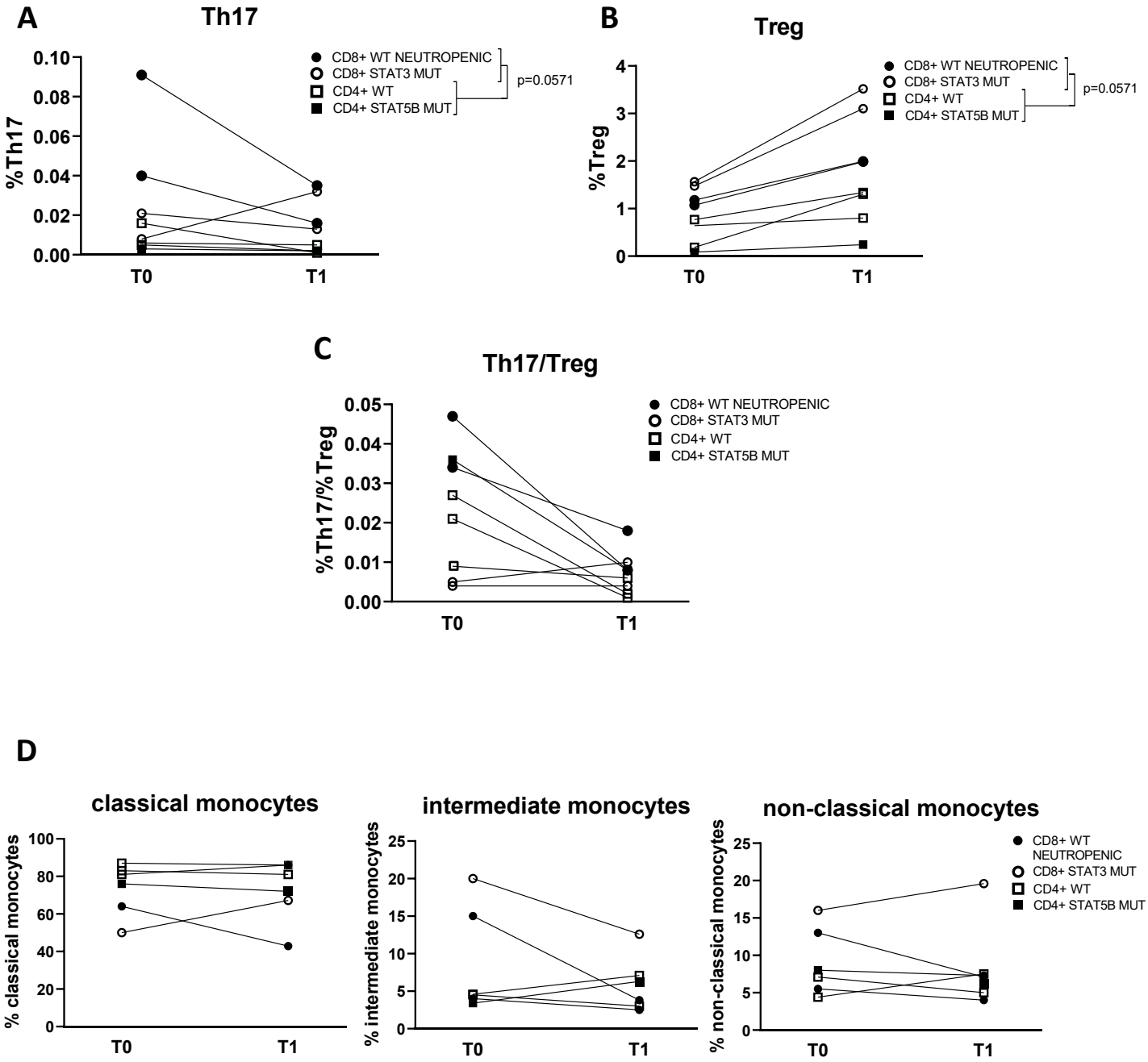

Supplemental Figure 8: Follow up evaluation of Th17, Treg and monocytes distribution in peripheral blood of T-LGLL patients. The percentage of Th17 and Treg (**A** and **B**, respectively) were evaluated by flow cytometry at baseline (T0) and at follow up (T1). The related Th17/Treg ratio was reported in panel C. Data obtained from 2 CD8+ wt neutropenic, 2 CD8+ *STAT3* mutated, 3 CD4+ wt and 1 CD4+ *STAT5B* mutated T-LGLL patients were analyzed by Mann-Whitney test after the clusterization for CD8 (n=4) or CD4 (n=4) positivity and reported in a "before and after" plot. (**D**) The percentage of classic, intermediate and non-classic monocytes was assessed by flow cytometry, at T0 and T1, in 1 CD8+ wt neutropenic, 1 CD8+ *STAT3* mutated, 3 CD4+ wt and 1 CD4+ *STAT5B* mutated T-LGLL patients. Data are reported in a before and after plot. No statistical evaluations were performed for the reduced number of statical units evaluated.

Supplemental Figure 9

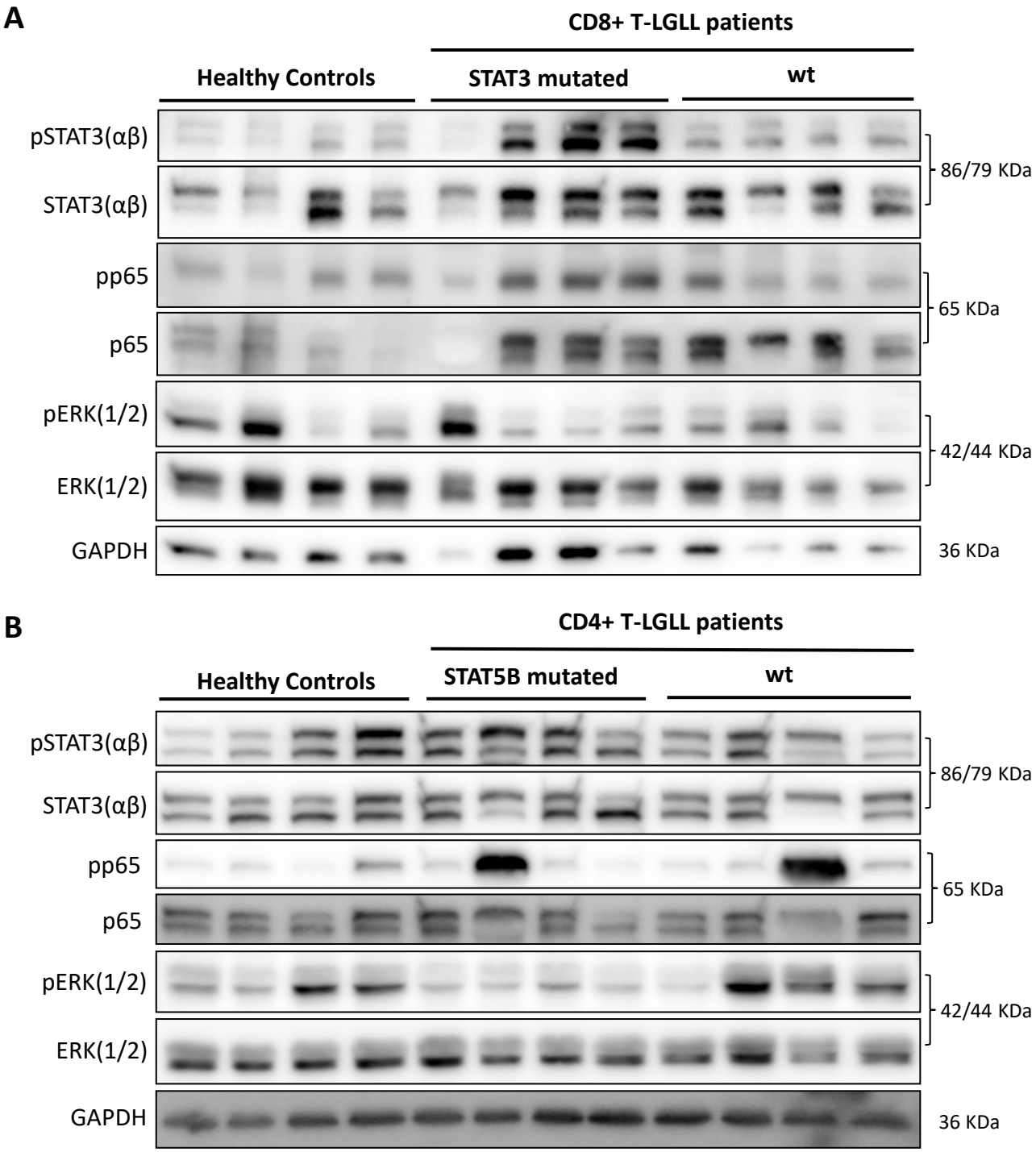

Supplemental Figure 9: Western Blot (WB) analysis of purified monocytes. WB images obtained from purified monocytes are reported for four representative healthy controls, CD8+ *STAT3* mutated and wt cases (**A**) and CD4+ *STAT5B* mutated and wt patients (**B**). The level of the protein phosphorylation (p) and expression for STAT3, p65 (the upper band on the image) and ERK have been evaluated for each sample analyzed. The level of expression of GAPDH has been used as loading control. KDa (Kilo Dalton)

Supplemental Figure 10

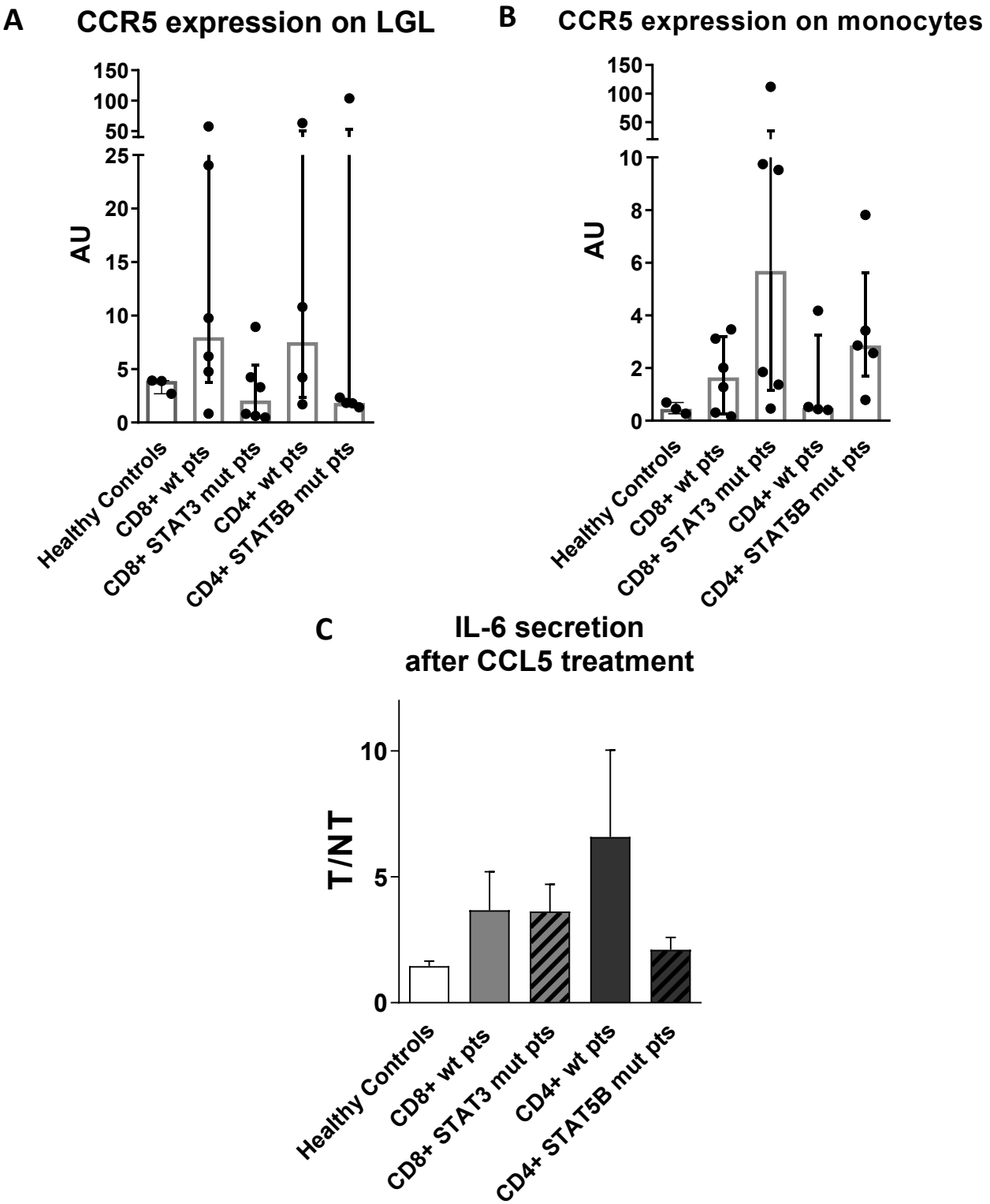

Supplemental Figure 10: Evaluation of monocytes and leukemic T-LGL communication. (**A-B**) CCR5 expression was assessed by RT-qPCR on immune-magnetically purified LGL (A) or monocytes (B) from 3 healthy controls 6 CD8+ wt, 6 CD8+ *STAT3* mutated, 4 CD4+ wt and 5 CD4+ *STAT5B* mutated T-LGLL patients. Results are reported as arbitrary units (AU). (**C**) Evaluation of IL-6 induction expression in immuno-magnetically purified monocytes cultured 12 hours under CCL5 stimulation (100 ng/ml) by ELISA. Results are represented as the ratio between the treated over the not treated conditions (T/NT). A slightly higher IL-6 secretion was observed for each T-LGLL subgroups (3 CD8+ wt, 4 CD8+ *STAT3* mutated, 5 CD4+ wt and 4 CD4+ *STAT5B* mutated) in comparison to healthy controls (n=7).

Supplemental Figure 11

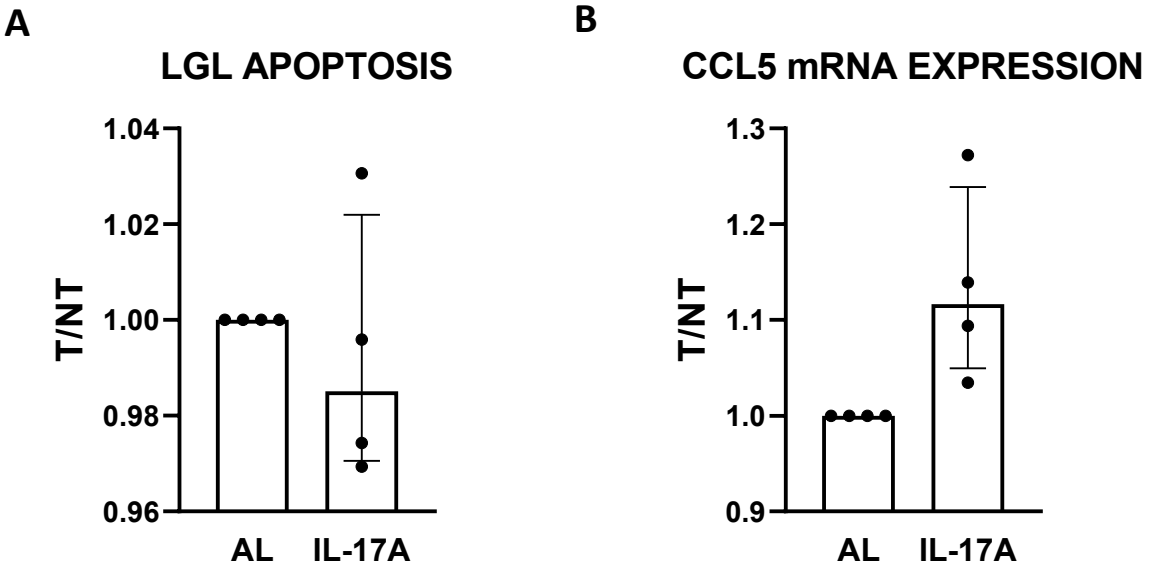

Supplemental figure 11: Immuno-magnetically purified LGLs, obtained from 4 CD8+ T-LGLL patients, were cultured 24 hours under IL-17A stimulation (100 ng/ml). Apoptosis was evaluated by annexin V staining (A) and CCL5 expression was evaluated by RT-qPCR (B). Data are reported as histograms showing median ratio between treated and not treated conditions (T/NT) with IQR and were analyzed by Mann-Whitney test.